

Reciprocity Calibration of Dual-Antenna Repeaters

Erik G. Larsson*, Joao Vieira†, and Pål Frenger‡

Abstract—We present a reciprocity calibration method for dual-antenna repeaters in wireless networks. The method uses bi-directional measurements between two network nodes, A and B, where for each bi-directional measurement, the repeaters are configured in different states. The nodes A and B could be two access points in a distributed MIMO system, or they could be a base station and a mobile user terminal, for example. From the calibration measurements, the differences between the repeaters’ forward and reverse gains are estimated. The repeaters are then (re-)configured to compensate for these differences such that the repeaters appear, transparently to the network, as reciprocal components of the propagation environment, enabling reciprocity-based beamforming in the network.

Index Terms—repeater, full-duplex relay, reciprocity, calibration.

I. INTRODUCTION

A. Repeaters

In wireless systems, most resources are typically used to serve disadvantaged users that have low path gains to the base station (access point). Such users may be in a shadowed area of the cell, or located indoors while the base station is located outdoors. In addition, such users typically see channels with low, or even unit, rank – prohibiting the transmission of more than a single data stream.

One technique for improving service to disadvantaged users is to use *repeaters* that amplify and instantaneously re-transmit the signal [1]–[7]. Repeaters, also known as full-duplex relays, have a small form-factor, and are relatively inexpensive to build and deploy. They pose, unlike access points in distributed MIMO, no requirements on phase coherency between geographically separated units.

Single-antenna repeaters use the same antenna for reception and transmission, and require a circulator to isolate the antenna, the transmitter port, and the receiver port – something considered challenging to implement. *Dual-antenna repeaters* have two antenna ports, one for transmission and one for reception. They have been standardized in 3GPP, in the form of network-controlled repeaters [8], and typically have a donor (pickup) antenna outdoors and an antenna indoors to provide coverage.

Our focus is on dual-antenna repeaters. These repeaters have one antenna that transmits on uplink and receives on downlink, and one that does the opposite, regardless of the duplexing mode. The first antenna is linked, via a forward

path with amplification, to the second antenna; the second antenna is linked, via a reverse path with amplification, to the first antenna. In TDD operation, the roles of the repeater’s antennas alternate over time according to the network’s TDD pattern. The repeater implementations we envision introduce no appreciable delay. All that is required is an amplifier circuit in either direction, a tunable amplitude- and phase-compensation RF circuit, and a control channel connection (in-band or in a separate band). Also, unless its antennas are separated sufficiently far apart, the repeater would need either internal echo cancellation circuitry, or a switch synchronized with the TDD pattern.

B. Reciprocity and Reciprocity Calibration

When operating a MIMO system in TDD, the reciprocity of the uplink-downlink channels facilitates the use of uplink pilots to acquire downlink channel state information.

The reciprocity principle for electromagnetic wave propagation states that for two antennas A_1 and A_2 in a linear-time invariant medium, a voltage at A_2 due to a current source at A_1 equals the voltage at A_1 due to the same current source at A_2 [9, p. 119]. When each of A_1 and A_2 is connected to a circuit, one then defines the transmitted and received signals, in both directions, as voltages at specified points in these circuits. The relation between these signals constitutes the [communication-theoretic] channel and it is also reciprocal (equal in both directions); in some cases (strong coupling, non-identical antennas), a linear transformation that depends on the circuit impedances is first required to guarantee that [10].

In practice, the transmitted and received signals will be affected by analog components whose phase-lag is slightly temperature- and age-dependent. Also, if different antennas are driven by different oscillators that are not phase-locked (common in distributed MIMO), their phases will drift apart over time. These two phenomena cause a non-reciprocity effect that is well modeled, for each antenna (indexed by n , say), by a time-varying complex-valued coefficient per receive and transmit branch, herein termed reciprocity coefficient and denoted by r_n and t_n . These coefficients must be tracked, and compensated for, to maintain uplink-downlink channel reciprocity; herein, this is called reciprocity calibration. The modeling with two coefficients per antenna branch is an approximation that assumes negligible cross-branch leakage, but has strong experimental support; see, e.g., [11]–[13].

Said non-reciprocity is present in base stations transceivers. It may also be present in dual-antenna repeaters – causing their forward and reverse gains to differ (note that their signal gain depends on the momentary link direction). For base stations, many schemes for estimation of $\{r_n, t_n\}$ exist; they typically

This work was supported by the European Union’s Horizon 2020 research and innovation programme under grant agreement No 101013425 (REINDEER), the KAW Foundation, and ELLIIT. *Linköping University, Dept. of Electrical Engineering (ISY), 581 83 Linköping, Sweden, erik.g.larsson@liu.se. †Ericsson Research, Mobilvägen 12, 223 62 Lund, Sweden, joao.vieira@ericsson.com. ‡Ericsson Research, Datalinjen 4, 581 12 Linköping, Sweden, pal.frenger@ericsson.com.

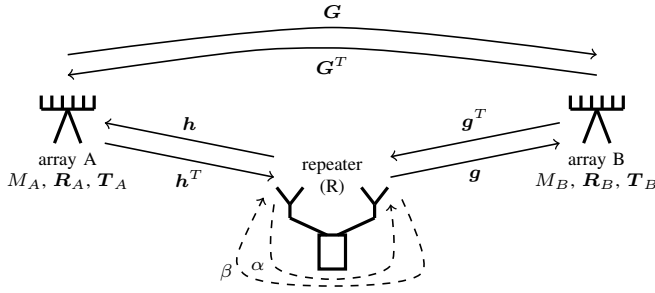


Fig. 1. Two antenna arrays, A and B, and a repeater (R). By definition, \mathbf{G} is the propagation channel from A to B with R turned off. Radio channels are represented by solid lines (—) and repeater gains by dashed lines (---).

rely on bi-directional over-the-air inter-antenna measurements, see, e.g., [11]–[15] (for co-located MIMO) [16], [17] (for distributed MIMO). None of those methods can be directly used for reciprocity calibration of repeaters, however.

C. Paper Contribution: Reciprocity-Calibration of Repeaters

We devise a method of calibrating nominally non-reciprocal dual-antenna repeaters, estimating the relation between their forward and reverse path gains (to be denoted α and β). Knowing this relation, the repeaters can be re-configured by sending them instructions over a control channel, such that their forward and reverse gains become equal. This causes the repeaters to appear as reciprocal parts of the propagation environment, entirely transparent to base stations and the users, making them useful network components in multiuser TDD systems that employ reciprocity-based beamforming.

To the authors' knowledge, there is no previous work on reciprocity calibration of repeaters. But it is worth pointing out that previous literature has identified the non-reciprocity of repeaters to be an important limitation of their potential to improve system performance [7]. Somewhat related is [18]; the authors consider the impact of reciprocity errors of relays (not repeaters), for which the system model is different.

II. SYSTEM MODEL

We consider a system with two antenna arrays, A and B, and a dual-antenna repeater, R. See Figure 1. The arrays A and B have M_A and M_B antennas, respectively. In practice, A and B could be a base station and a mobile, or two access points, for example.

We denote the $M_B \times M_A$ propagation channel from A to B, when R is turned off, by \mathbf{G} . Reciprocity of propagation holds so the channel from B to A is \mathbf{G}^T . No other assumptions are made on the \mathbf{G} ; it could include both line-of-sight and multipath components. Note that \mathbf{G} includes the “passive” effects of R: even when it is turned off, R may scatter impinging waves and behave as a (substantially) reciprocal entity. We model the non-reciprocity of the transmit and receive branches at A and B via four diagonal matrices: \mathbf{R}_A , \mathbf{T}_A , \mathbf{R}_B , and \mathbf{T}_B , comprising the reciprocity coefficients $\{r_{An}, t_{An}, r_{Bn}, t_{Bn}\}$ introduced in Section I-B.

We denote the $1 \times M_A$ propagation channel from A to R by \mathbf{h}^T , and the $M_A \times 1$ reverse channel from R to A by

\mathbf{h} .¹ Similarly, we denote the channel from B to R by \mathbf{g}^T and the reverse channel by \mathbf{g} . When R is in its nominal configuration, we denote the (complex-valued) gains of its forward and reverse paths by α and β . Generally, $\alpha \neq \beta$; the repeater may nominally not be reciprocal.

Taken together, including the reciprocity coefficients in the model, the (noise-free) channel from A to B is $\mathbf{R}_B(\mathbf{G} + \alpha\mathbf{g}\mathbf{h}^T)\mathbf{T}_A$ and the channel from B to A is $\mathbf{R}_A(\mathbf{G}^T + \beta\mathbf{h}\mathbf{g}^T)\mathbf{T}_B$.

For generality, none of the arrays, A or B, is assumed to be a priori reciprocity-calibrated. Hence, α , β , \mathbf{G} , \mathbf{g} and \mathbf{h} , \mathbf{R}_A , \mathbf{T}_A , \mathbf{R}_B and \mathbf{T}_B are a priori unknown.

III. CALIBRATION SCHEME

Our scheme takes two bi-directional measurements between A and B: (1) one uni-directional measurement from A to B along with one from B to A with R in a *nominal configuration*; and (2) one uni-directional measurement from A to B along with one from B to A with R *configured to rotate the phase of its forward and reverse gains by π* . These measurements are taken within a single channel coherence time interval, by transmitting pre-determined pilots in a standard manner. This gives the four channel estimates,

$$\mathbf{X}_{AB}^0 = \mathbf{R}_B(\mathbf{G} + \alpha\mathbf{g}\mathbf{h}^T)\mathbf{T}_A + \mathbf{W}_B^0, \quad (M_B \times M_A) \quad (1)$$

$$\mathbf{X}_{BA}^0 = \mathbf{R}_A(\mathbf{G}^T + \beta\mathbf{h}\mathbf{g}^T)\mathbf{T}_B + \mathbf{W}_A^0, \quad (M_A \times M_B) \quad (2)$$

$$\mathbf{X}_{AB}^1 = \mathbf{R}_B(\mathbf{G} - \alpha\mathbf{g}\mathbf{h}^T)\mathbf{T}_A + \mathbf{W}_B^1, \quad (M_B \times M_A) \quad (3)$$

$$\mathbf{X}_{BA}^1 = \mathbf{R}_A(\mathbf{G}^T - \beta\mathbf{h}\mathbf{g}^T)\mathbf{T}_B + \mathbf{W}_A^1, \quad (M_A \times M_B) \quad (4)$$

where \mathbf{W}_x^\times represents measurement noise.

The objective is to estimate α and β , so all other unknowns are nuisance parameters – parameters present in the model but of no interest. The problem of estimating α and β turns out to be non-identifiable, but the ratio β/α can be estimated and this is sufficient to calibrate the repeater in order to make it reciprocal. Specifically, once β/α has been estimated, the repeater can be instructed to adjust its forward or reverse path gains such that after the adjustment, these gains are equal.

A. An Ingenious Approach to Estimation of β/α

Absent noise, we have from (1)–(4) that,

$$2\mathbf{X}_{AB}^0 \oslash (\mathbf{X}_{AB}^0 + \mathbf{X}_{AB}^1) - \mathbf{1}\mathbf{1}^T = -\alpha(\mathbf{g}\mathbf{h}^T) \oslash \mathbf{G}, \quad (5)$$

$$\left[2\mathbf{X}_{BA}^0 \oslash (\mathbf{X}_{BA}^0 + \mathbf{X}_{BA}^1) - \mathbf{1}\mathbf{1}^T \right]^T = -\beta(\mathbf{g}\mathbf{h}^T) \oslash \mathbf{G}, \quad (6)$$

where \oslash denotes element-wise (Hadamard) division and $\mathbf{1} = [1, \dots, 1]^T$. Dividing (6) by (5) we see that

$$\left[2\mathbf{X}_{BA}^0 \oslash (\mathbf{X}_{BA}^0 + \mathbf{X}_{BA}^1) - \mathbf{1}\mathbf{1}^T \right]^T \oslash \left[2\mathbf{X}_{AB}^0 \oslash (\mathbf{X}_{AB}^0 + \mathbf{X}_{AB}^1) - \mathbf{1}\mathbf{1}^T \right] = \frac{\beta}{\alpha}\mathbf{1}\mathbf{1}^T. \quad (7)$$

This observation suggests that one could estimate β/α by averaging the elements of the left hand side of (7). The resulting estimate gives the correct result in the noise-free case, but it is statistically unsound because of the division by $\mathbf{X}_{BA}^0 + \mathbf{X}_{BA}^1$, which can be small. For example, suppose \mathbf{G} is

¹By convention, throughout, all vectors are column vectors.

Rayleigh fading with i.i.d. $CN(0, 1)$ elements, and that there is no noise. Then the elements of $\mathbf{X}_{BA}^0 \oslash (\mathbf{X}_{BA}^0 + \mathbf{X}_{BA}^1)$ have undefined moments.² As a consequence, the performance of this estimator will be erratic, and cannot even be determined reliably via Monte-Carlo simulation. So while this approach could appear tempting, it should not be used. The only purpose of discussing it here is to make this point.

B. Non-Linear Least Squares (NLS) Criterion

To tackle the estimation problem systematically, we start by re-parameterizing the problem, defining,

$$\mathbf{H} = \mathbf{R}_B \mathbf{G} \mathbf{T}_A, \quad \mathbf{A} = \mathbf{T}_A^{-1} \mathbf{R}_A, \quad \mathbf{B} = \mathbf{T}_B \mathbf{R}_B^{-1}, \quad (8)$$

$$\mathbf{Z} = \alpha \mathbf{R}_B \mathbf{g} \mathbf{h}^T \mathbf{T}_A, \quad \gamma = \frac{\beta}{\alpha}. \quad (9)$$

This re-parameterization is parsimonious, up to an irrelevant scaling ambiguity – as will be clear shortly. The channel estimates, expressed in the new variables, are

$$\mathbf{X}_{AB}^0 = \mathbf{H} + \mathbf{Z} + \mathbf{W}_B^0, \quad (10)$$

$$\mathbf{X}_{BA}^0 = \mathbf{A}(\mathbf{H} + \gamma \mathbf{Z})^T \mathbf{B} + \mathbf{W}_A^0, \quad (11)$$

$$\mathbf{X}_{AB}^1 = \mathbf{H} - \mathbf{Z} + \mathbf{W}_B^1, \quad (12)$$

$$\mathbf{X}_{BA}^1 = \mathbf{A}(\mathbf{H} - \gamma \mathbf{Z})^T \mathbf{B} + \mathbf{W}_A^1. \quad (13)$$

A least-squares estimator, which also yields the maximum-likelihood solution if all noise components are i.i.d. zero-mean Gaussian, entails minimizing the criterion,

$$f = \|\mathbf{X}_A^0 - \mathbf{H} - \mathbf{Z}\|^2 + \|\mathbf{X}_B^0 - \mathbf{A}(\mathbf{H} + \gamma \mathbf{Z})^T \mathbf{B}\|^2 + \|\mathbf{X}_A^1 - (\mathbf{H} - \mathbf{Z})\|^2 + \|\mathbf{X}_B^1 - \mathbf{A}(\mathbf{H} - \gamma \mathbf{Z})^T \mathbf{B}\|^2 \quad (14)$$

with respect to \mathbf{H} , \mathbf{A} , \mathbf{B} , \mathbf{Z} and γ , subject to the constraints that \mathbf{A} and \mathbf{B} are diagonal, and that \mathbf{Z} has unit rank. Hereafter, $\|\cdot\|$ denotes the Frobenius norm. The above-mentioned ambiguity is now obvious: multiplication of \mathbf{A} by an arbitrary constant and division of \mathbf{B} by the same constant yields no change in the objective (14). But apart from this ambiguity, all parameters are identifiable.

C. Basic NLS Fitting Algorithm

A straightforward calculation shows that (14) can be equivalently written as

$$f = \|\mathbf{R}_1 - \mathbf{H}\|^2 + \|\mathbf{R}_2 - \mathbf{Z}\|^2 + \left\| \mathbf{R}_3 - \mathbf{A} \mathbf{H}^T \mathbf{B} \right\|^2 + \left\| \mathbf{R}_4 - \gamma \mathbf{A} \mathbf{Z}^T \mathbf{B} \right\|^2, \quad (15)$$

where we defined the following pre-processed measurements:

$$\mathbf{R}_1 = \frac{1}{2}(\mathbf{X}_{AB}^0 + \mathbf{X}_{AB}^1), \quad \mathbf{R}_2 = \frac{1}{2}(\mathbf{X}_{AB}^0 - \mathbf{X}_{AB}^1),$$

$$\mathbf{R}_3 = \frac{1}{2}(\mathbf{X}_{BA}^0 + \mathbf{X}_{BA}^1), \quad \mathbf{R}_4 = \frac{1}{2}(\mathbf{X}_{BA}^0 - \mathbf{X}_{BA}^1).$$

To approximately find the minimizers of (15) we perform the following sequential algorithmic steps:

²To see this, let x and y be independent $CN(0, 1)$. Then $|x|$ and $|y|$ are independent Rayleigh, and $|x/y| \geq 1/|y|$ with positive probability. A direct calculation shows that $\text{var}[1/y] = \infty$, so $\text{var}[x/y] = \infty$.

- 1) Minimize the first term of (15) with respect to \mathbf{H} :

$$\hat{\mathbf{H}} = \mathbf{R}_1. \quad (16)$$

- 2) Minimize the second term of (15) with respect to \mathbf{Z} . This gives

$$\hat{\mathbf{Z}} = \mathcal{S}\{\mathbf{R}_2\}, \quad (17)$$

where $\mathcal{S}\{\cdot\}$ is the best rank-one approximation of a matrix in the least-squares sense (the dominant term in the singular-value decomposition).

- 3) Insert $\hat{\mathbf{H}}$ for \mathbf{H} into (15), and minimize the third term with respect to \mathbf{A} and \mathbf{B} . This can be done by alternating projection with respect to \mathbf{A} and \mathbf{B} . Specifically, initialize $\hat{\mathbf{A}} = \hat{\mathbf{B}} = \mathbf{I}$.³ Then iterate the following two steps, a pre-determined number of steps or until the decrease in the objective $\|\mathbf{R}_3 - \mathbf{A} \hat{\mathbf{H}}^T \mathbf{B}\|$ falls below a threshold:

$$\hat{\mathbf{A}}_{ii} = \frac{(\hat{\mathbf{B}} \hat{\mathbf{H}})_i^H (\mathbf{R}_3)_i}{\|(\hat{\mathbf{B}} \hat{\mathbf{H}})_i\|^2}, \quad \hat{\mathbf{B}}_{ii} = \frac{(\hat{\mathbf{A}} \hat{\mathbf{H}}^T)_i^H (\mathbf{R}_3)_i}{\|(\hat{\mathbf{A}} \hat{\mathbf{H}}^T)_i\|^2},$$

for all i , where $(\cdot)_i$ denotes the i th column of a matrix. In this iteration, the objective is non-increasing, and non-negative, so it converges. Because of the scalar ambiguity between \mathbf{A} and \mathbf{B} , to ensure numerical stability (avoid that $\hat{\mathbf{A}}$ shrinks and $\hat{\mathbf{B}}$ grows, or vice versa), it is sound practice to normalize $\hat{\mathbf{A}}$ and $\hat{\mathbf{B}}$ in every iteration, for example, such that $\|\mathbf{A}\|^2 = 1$.

- 4) Insert $\hat{\mathbf{H}}$, $\hat{\mathbf{A}}$, $\hat{\mathbf{B}}$ and $\hat{\mathbf{Z}}$ into (15), and minimize the last term with respect to γ :

$$\hat{\gamma} = \frac{\text{Tr}\{(\hat{\mathbf{A}} \hat{\mathbf{Z}}^T \hat{\mathbf{B}})^H \mathbf{R}_4\}}{\|\hat{\mathbf{A}} \hat{\mathbf{Z}}^T \hat{\mathbf{B}}\|^2}. \quad (18)$$

D. Improving the Estimate by Alternating Optimization

One can improve the above estimate by alternating optimization, iterating the following steps:

- 1) Insert $\hat{\mathbf{A}}$, $\hat{\mathbf{B}}$, $\hat{\mathbf{Z}}$ and $\hat{\gamma}$, and minimize (15) with respect to \mathbf{H} . Letting

$$\mathbf{x} = \begin{bmatrix} \text{vec}\{\mathbf{R}_1\} \\ \text{vec}\{\mathbf{R}_3\} \end{bmatrix}, \quad \mathbf{F} = \begin{bmatrix} \mathbf{I}_{M_A} \otimes \mathbf{I}_{M_B} \\ \hat{\mathbf{A}} \otimes \hat{\mathbf{B}} \end{bmatrix},$$

where \otimes denotes the Kronecker product, and $\text{vec}\{\cdot\}$ denotes the stacking of the columns of a matrix on top of one another, we obtain

$$\text{vec}\{\hat{\mathbf{H}}\} = (\mathbf{F}^H \mathbf{F})^{-1} \mathbf{F}^H \mathbf{x}.$$

- 2) Insert $\hat{\mathbf{H}}$ into (15) and minimize with respect to \mathbf{A} and \mathbf{B} , by iterating the following steps:

$$\hat{\mathbf{A}}_{ii} = \frac{(\hat{\mathbf{B}} \hat{\mathbf{H}})_i^H (\mathbf{R}_3)_i + \hat{\gamma}^* (\hat{\mathbf{B}} \hat{\mathbf{Z}})_i^H (\mathbf{R}_4)_i}{\|(\hat{\mathbf{B}} \hat{\mathbf{H}})_i\|^2 + |\hat{\gamma}|^2 \|(\hat{\mathbf{B}} \hat{\mathbf{Z}})_i\|^2},$$

³Other initializations are possible. For example, if there is no noise then $(\mathbf{X}_{BA}^0 + \mathbf{X}_{BA}^1)^T \oslash (\mathbf{X}_{AB}^0 + \mathbf{X}_{AB}^1)$ has rank one, and its left and right singular vectors are proportional to the diagonals of \mathbf{B} and \mathbf{A}^* . These could be taken as initial point. However, as noted in Section III-A, element-wise division should be avoided.

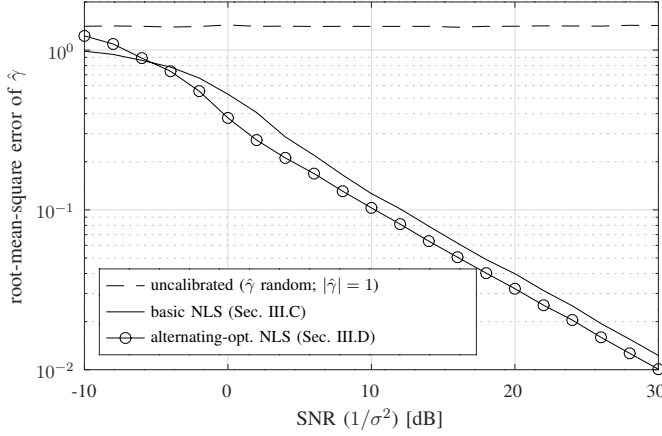


Fig. 2. Root-mean-square-error of $\hat{\gamma}$.

$$\hat{B}_{ii} = \frac{(\hat{A}\hat{H}^T)_i^H(\mathbf{R}_3)_i + \hat{\gamma}^*(\hat{A}\hat{Z}^T)_i^H(\mathbf{R}_4)_i}{\|(\hat{A}\hat{H}^T)_i\|^2 + |\hat{\gamma}|^2\|(\hat{A}\hat{Z}^T)_i\|^2}.$$

- 3) Insert \hat{A} , \hat{B} , \hat{H} and $\hat{\gamma}$ into (15) and minimize with respect to \mathbf{Z} . The exact minimum is elusive to us. We suggest an approximate solution given by the best rank-one fit to a linear combination of \mathbf{R}_2 and $\hat{B}^{-1}\mathbf{R}_4^T\hat{A}^{-1}$:

$$\hat{Z} = S \left\{ \frac{\mathbf{R}_2 + \hat{\gamma}^*\hat{B}^{-1}\mathbf{R}_4^T\hat{A}^{-1}}{1 + |\hat{\gamma}|^2} \right\}. \quad (19)$$

- 4) Insert \hat{A} , \hat{B} , \hat{H} and \hat{Z} into (15) and minimize with respect to γ ; the resulting $\hat{\gamma}$ is given by (18).
 5) Repeat from step 1), a pre-determined number of times or until the objective (15) no longer decreases.

Our proposed NLS fit is statistically sound as it gives the maximum-likelihood solution in white Gaussian noise. Better algorithms for minimizing the objective (15) might, however, exist. In the basic NLS fitting algorithm in Section III-C, the obtained estimates $(\hat{H}, \hat{Z}, \hat{A}, \hat{B}, \hat{\gamma})$ are approximate since no attempt is made to find the global minimum of (15). However, the algorithm is computationally very simple, and yields consistent estimates in the case of vanishing noise (to show this, note that $\hat{H} \rightarrow H$, $\hat{Z} \rightarrow Z$, and so forth). The alternating optimization in Section III-D yields estimates that are closer to the global optimum of (15). However, since \hat{Z} in (19) is an approximate minimizer, there is no guarantee that the objective is non-increasing in every iteration. To ensure that the algorithm does not “derail”, we terminate the iteration in case the objective would increase (which can happen because of said approximation).

IV. NUMERICAL EXAMPLE

We consider an example where A has $M_A = 4$ antennas and B has $M_B = 3$ antennas. The vectors \mathbf{h} and \mathbf{g} are random columns of $M_A \times M_A$ and $M_B \times M_B$ DFT matrices, modeling line-of-sight propagation between A and R and between R and B. The propagation channel between A and B with R off, \mathbf{G} , has independent $CN(0, 1)$ entries, modeling Rayleigh

fading. The diagonal entries of \mathbf{R}_A , \mathbf{T}_A , \mathbf{R}_B and \mathbf{T}_B have unit magnitudes, and independent, uniformly random phases over $[-\pi, \pi]$. The noise matrices \mathbf{W}_A^0 , \mathbf{W}_B^0 , \mathbf{W}_A^1 , and \mathbf{W}_B^1 have independent $CN(0, \sigma^2)$ elements; $1/\sigma^2$ is the SNR as measured at any antenna of B when one antenna at A transmits with unit power and R is off.

Figure 2 shows the performance of the basic NLS and alternating-optimization NLS estimators, for repeater gains $|\alpha|^2 = |\beta|^2 = 10$ dB. 100 iterations were run in the alternating projection subroutines that minimize with respect to \mathbf{A} and \mathbf{B} (Step 3 in Section III-C and Step 2 in Section III-D). At high SNR, the root-mean-square error decreases by approximately a factor 10 when increasing the SNR 20 dB. This is expected, as for non-linear models with additive white Gaussian noise, the curvature of the log-likelihood is proportional to the SNR. The alternating optimization in Section III-D was run for at most 25 iterations; it improves performance almost 2 dB, at the cost of correspondingly higher complexity.

V. VARIATIONS AND EXTENSIONS

A. Pre-Calibrated Arrays

If A and B have been previously reciprocity-calibrated, for example using the technique in [16], then \mathbf{A} and \mathbf{B} can be considered known. The above algorithm substantially simplifies in this case, as the only unknowns are γ , \mathbf{H} and \mathbf{Z} ; we leave the details to the reader. However, we stress that this requires A and B to be *jointly* reciprocity-calibrated. Individual calibration is insufficient – for an explanation of the difference, see [17]. For example, if A and B are driven by independent oscillators, then re-calibration of A and B for joint reciprocity must be done every time the oscillators have drifted apart by more than some predefined angle.

B. Turning On and Off Instead of Phase-Shifting

Instead of performing one bi-directional measurement with R in a nominal configuration and one bi-directional measurement instructing R to phase-shift by π , one can take one such measurement with R on and one with R off. We get the two bi-directional measurements (ignoring noise henceforth for simplicity):

$$\mathbf{Y}_{AB}^0 = \mathbf{H} + \mathbf{Z}, \quad \mathbf{Y}_{BA}^0 = \mathbf{A}(\mathbf{H} + \gamma\mathbf{Z})^T\mathbf{B}, \quad (20)$$

$$\mathbf{Y}_{AB}^1 = \mathbf{H}, \quad \mathbf{Y}_{BA}^1 = \mathbf{A}\mathbf{H}^T\mathbf{B}. \quad (21)$$

The NLS criterion in (14) can be easily modified to this case, resulting in similar algorithms as in Section III.

C. Simultaneous Calibration of Multiple Repeaters

With multiple repeaters in the network, their operation needs to be coordinated during calibration activities. One can of course, trivially, calibrate one repeater at a time by turning off all but the one that is up for calibration. However, one can do better by instructing the repeaters to rotate the phase of their gains according to a pre-determined pattern. We exemplify this as follows, using phase rotations of 0 and π .

Consider a setup with N repeaters, R_1, \dots, R_N , with corresponding rank-one channels $\mathbf{Z}_1, \dots, \mathbf{Z}_N$ and gain ratios $\gamma_1, \dots, \gamma_N$. First, as an initial step, configure the repeaters to set their gains equal to a nominal value. This yields the (noise-free) bi-directional measurement

$$\mathbf{Y}_{AB}^0 = \mathbf{H} + \mathbf{Z}_1 + \dots + \mathbf{Z}_N, \quad (22)$$

$$\mathbf{Y}_{BA}^0 = \mathbf{A}(\mathbf{H} + \gamma_1 \mathbf{Z}_1 + \dots + \gamma_N \mathbf{Z}_N)^T \mathbf{B}. \quad (23)$$

Next, configure all repeaters to rotate the phase of their gains by π , resulting in the bi-directional measurement

$$\mathbf{Y}_{AB}^1 = \mathbf{H} - \mathbf{Z}_1 - \dots - \mathbf{Z}_N, \quad (24)$$

$$\mathbf{Y}_{BA}^1 = \mathbf{A}(\mathbf{H} - \gamma_1 \mathbf{Z}_1 - \dots - \gamma_N \mathbf{Z}_N)^T \mathbf{B}. \quad (25)$$

From (22)–(25), $\mathbf{A}\mathbf{H}$ and $\mathbf{B}\mathbf{H}\mathbf{A}$ can be recovered (up to a multiplicative scalar ambiguity between \mathbf{A} and \mathbf{B}). For example, \mathbf{H} can be estimated by averaging \mathbf{Y}_{AB}^0 and \mathbf{Y}_{AB}^1 , and $\mathbf{B}\mathbf{H}\mathbf{A}$ can be estimated by averaging $(\mathbf{Y}_{BA}^0)^T$ and $(\mathbf{Y}_{BA}^1)^T$. Consequently, any terms of the form \mathbf{H} or $\mathbf{B}\mathbf{H}\mathbf{A}$ that appear in subsequent measurements can be eliminated. From now on, we assume that such elimination has been performed. Also, we can assume that the diagonal matrices \mathbf{A} and \mathbf{B} are known (up to a multiplicative scalar ambiguity) since they can be determined from \mathbf{H} and $\mathbf{B}\mathbf{H}\mathbf{A}$.

After this initial step, instruct the repeaters to rotate their phases according to a pre-determined pattern. We give an example, for $N = 4$, using a pattern from a Hadamard matrix. For each pattern, bi-directional measurements are taken. This yields, after subtracting the already-obtained estimates of \mathbf{H} and $\mathbf{B}\mathbf{H}\mathbf{A}$, and after transposition:

$$\mathbf{Z}_1 + \mathbf{Z}_2 + \mathbf{Z}_3 + \mathbf{Z}_4 \quad (26)$$

$$\mathbf{B}(\gamma_1 \mathbf{Z}_1 + \gamma_2 \mathbf{Z}_2 + \gamma_3 \mathbf{Z}_3 + \gamma_4 \mathbf{Z}_4) \mathbf{A} \quad (27)$$

$$\mathbf{Z}_1 - \mathbf{Z}_2 + \mathbf{Z}_3 - \mathbf{Z}_4 \quad (28)$$

$$\mathbf{B}(\gamma_1 \mathbf{Z}_1 - \gamma_2 \mathbf{Z}_2 + \gamma_3 \mathbf{Z}_3 - \gamma_4 \mathbf{Z}_4) \mathbf{A} \quad (29)$$

$$\mathbf{Z}_1 + \mathbf{Z}_2 - \mathbf{Z}_3 - \mathbf{Z}_4 \quad (30)$$

$$\mathbf{B}(\gamma_1 \mathbf{Z}_1 + \gamma_2 \mathbf{Z}_2 - \gamma_3 \mathbf{Z}_3 - \gamma_4 \mathbf{Z}_4) \mathbf{A} \quad (31)$$

$$\mathbf{Z}_1 - \mathbf{Z}_2 - \mathbf{Z}_3 + \mathbf{Z}_4 \quad (32)$$

$$\mathbf{B}(\gamma_1 \mathbf{Z}_1 - \gamma_2 \mathbf{Z}_2 - \gamma_3 \mathbf{Z}_3 + \gamma_4 \mathbf{Z}_4) \mathbf{A}. \quad (33)$$

Note that (26) and (27) were already obtained in the initial step when \mathbf{H} and $\mathbf{B}\mathbf{H}\mathbf{A}$ were estimated; we repeat them here for completeness. Once \mathbf{A} and \mathbf{B} are estimated, by forming linear combinations (26)–(33), we can recover $\{\mathbf{Z}_n\}$ and $\{\gamma_n \mathbf{B}\mathbf{Z}_n \mathbf{A}\}$ by inverting the Hadamard pattern, and then recover $\{\gamma_n\}$. For example, adding (26), (28), (30), and (32) yields $4\mathbf{Z}_1$. Adding (27), (29), (31), and (33) yields $4\gamma_1 \mathbf{B}\mathbf{Z}_1 \mathbf{A}$. Since \mathbf{A} and \mathbf{B} are known, γ_1 can then be found from these two sums. Similarly, by forming other linear combinations of (26)–(33), $\gamma_2, \dots, \gamma_4$ can be determined.

Other constructions, for example based on DFT matrices, are also possible. Orthonormal patterns are preferable, as they yield a well-conditioned inversion in the last step.

VI. CONCLUDING REMARKS

The potential of using repeaters to enhance performance of reciprocity-based multiuser MIMO has been discounted

in the past because their presence, nominally, breaks the uplink-downlink reciprocity. With our proposed reciprocity calibration technique, dual-antenna repeaters can be made into transparent, reciprocal components of the radio wave propagation environment – enabling improved multiplexing capability and improved coverage to disadvantaged users.

Our scheme requires a reasonable SNR on the direct link (with the repeater off) to achieve good-quality estimates. In a deployment with many repeaters, as long as one can calibrate a first repeater, one could use it to calibrate a second repeater, even if there is no good direct-link to calibrate this second repeater, and so on.

REFERENCES

- [1] M. N. Patwary, P. B. Rapajic, and I. Oppermann, "Capacity and coverage increase with repeaters in UMTS urban cellular mobile communication environment," *IEEE Transactions on Communications*, vol. 53, no. 10, pp. 1620–1624, 2005.
- [2] S. K. Sharma, M. Patwary, S. Chatzinotas, B. Ottersten, and M. Abdel-Maguid, "Repeater for 5G wireless: A complementary contender for spectrum sensing intelligence," in *IEEE ICC*, 2015, pp. 1416–1421.
- [3] M. Garcia-Lozano, L. Alonso, F. Casadevall, S. Ruiz, and L. M. Correia, "Enhanced analysis of WCDMA networks with repeaters deployment," *IEEE Transactions on Wireless Communications*, vol. 6, no. 9, pp. 3429–3439, 2007.
- [4] L.-S. Tsai and D.-S. Shiu, "Capacity scaling and coverage for repeater-aided MIMO systems in line-of-sight environments," *IEEE Transactions on Wireless Communications*, vol. 9, no. 5, pp. 1617–1627, 2010.
- [5] R. A. Ayoubi, M. Mizmizi, D. Tagliaferri, D. De Donno, and U. Spagnolini, "Network-controlled repeaters vs. reconfigurable intelligent surfaces for 6G mmW coverage extension: A simulative comparison," in *IEEE MedComNet*, 2023.
- [6] G. Leone, E. Moro, I. Filippini, A. Capone, and D. De Donno, "Towards reliable mmWave 6G RAN: Reconfigurable surfaces, smart repeaters, or both?" in *IEEE WiOpt*, 2022.
- [7] Y. Ma, D. Zhu, B. Li, and P. Liang, "Channel estimation error and beamforming performance in repeater-enhanced massive MIMO systems," in *IEEE PIMRC*, 2015, pp. 672–677.
- [8] *3GPP TS 38.106, NR repeater radio transmission and reception*, 2022.
- [9] R. F. Harrington, *Time-Harmonic Electromagnetic Fields*. Wiley, 2001.
- [10] T. Laas, J. A. Nossek, S. Bazzi, and W. Xu, "On reciprocity in physically consistent TDD systems with coupled antennas," *IEEE Transactions on Wireless Communications*, vol. 19, no. 10, pp. 6440–6453, 2020.
- [11] J. Vieira, F. Rusek, O. Edfors, S. Malkowsky, L. Liu, and F. Tufvesson, "Reciprocity calibration for massive MIMO: Proposal, modeling, and validation," *IEEE Transactions on Wireless Communications*, vol. 16, no. 5, pp. 3042–3056, 2017.
- [12] X. Jiang, A. Decurninge, K. Gopala, F. Kaltenberger, M. Guillaud, D. Slock, and L. Deneire, "A framework for over-the-air reciprocity calibration for TDD massive MIMO systems," *IEEE Transactions on Wireless Communications*, vol. 17, no. 9, pp. 5975–5990, 2018.
- [13] C. Shepard, H. Yu, N. Anand, E. Li, T. Marzetta, R. Yang, and L. Zhong, "Argos: Practical many-antenna base stations," in *International Conference on Mobile Computing and Networking*, 2012.
- [14] F. Kaltenberger, J. Haiyong, M. Guillaud, and R. Knopp, "Relative channel reciprocity calibration in MIMO/TDD systems," in *Proc. Future Network and Mobile Summit*, Florence, Italy, June 2010.
- [15] B. M. Lee, "Calibration for channel reciprocity in industrial massive MIMO antenna systems," *IEEE Transactions on Industrial Informatics*, vol. 14, no. 1, pp. 221–230, 2017.
- [16] J. Vieira and E. G. Larsson, "Reciprocity calibration of distributed massive MIMO access points for coherent operation," in *IEEE PIMRC*, 2021.
- [17] E. G. Larsson and J. Vieira, "Phase calibration of distributed antenna arrays," *IEEE Communications Letters*, 2023.
- [18] R. Nie, L. Chen, N. Zhao, Y. Chen, F. R. Yu, and G. Wei, "Relaying systems with reciprocity mismatch: Impact analysis and calibration," *IEEE Transactions on Communications*, vol. 68, no. 7, pp. 4035–4049, 2020.